ABCG2 Expression and Side Population Abundance Regulated by a Transforming Growth Factor β–Directed Epithelial-Mesenchymal Transition

Liqun Yin, Paola Castagnino, and Richard K. Assoian

Department of Pharmacology, University of Pennsylvania School of Medicine, Philadelphia, Pennsylvania

Abstract

We describe here the regulation of ABCG2 expression and side population (SP) abundance in MCF7 human breast cancer cells. The level of ABCG2 mRNA and protein were increased in purified MCF7 SP relative to non-SP cells, and incubation with an ABCG2-specific inhibitor or ABCG2 short interfering RNA eliminated the MCF7 SP. The purified MCF7 SP could generate a heterogeneous population containing both SP and non-SP cells in culture. *In vivo* tumorigenicity experiments showed that the purified MCF7 SP has an increased ability to colonize the mouse mammary gland. Importantly, the MCF7 SP was depleted by a transforming growth factor-β (TGFβ)–directed epithelial-mesenchymal transition (EMT), and this effect was associated with a strong down-regulation of *ABCG2* gene expression, and an increased sensitivity to mitoxantrone. ABCG2 expression and SP abundance were restored upon the removal of transforming growth factor-β and reversion of the cells to an epithelial phenotype. Knock-down of E-cadherin also reduced SP abundance, but this effect was not accompanied by the loss of ABCG2 mRNA or protein. We conclude that ABCG2 expression in MCF7 cells is regulated during an EMT, and that the EMT effect reflects posttranslational regulation of ABCG2 function by E-cadherin as well as transcriptional repression of the *ABCG2* gene. [Cancer Res 2008;68(3):800–7]

Introduction

The ABC transporter family contains ~50 members which use the hydrolysis of ATP to pump toxins from cells (1, 2). ABC transporters probably play a physiologic role in detoxification, but the pathologic consequence of their action is that many chemotherapeutic agents are also effluxed by these transporters (3, 4). Two of the best studied ABC transporters are the multidrug resistance protein (called MDR1 or ABCB1) and the breast cancer resistance protein (called BCRP or ABCG2). These transporters have overlapping specificities for drug efflux. ABCG2 effluxes mitoxantrone, doxorubicin, certain camptothecins (topoisomerase inhibitors), and methotrexate (1, 5–8). One report indicates that ABCG2 may also protect cells from death associated with hypoxia (9).

ABC transporters also efflux Hoechst 33342 (10, 11). This property allows for the facile identification and sorting of ABC transporter-positive and transporter-negative cells by flow cytometry. In most cases, cells expressing ABC transporters comprise a very small percentage of freshly isolated cells, appearing as a "side population" (SP) relative to the majority of ABC transporter-negative cells (the non-SP) in Hoechst-based flow cytometry profiles (11–13). SPs, and especially ABCG2-dependent SPs, are seen in stem/progenitor cells (2, 3).

A hallmark of stem cells is that they can undergo symmetrical and asymmetrical cell division (14, 15). In symmetrical cell division, two identical daughter cells are produced (self-renewal), whereas asymmetrical cell division results in one daughter stem cell and one more differentiated progenitor cell. Asymmetrical cell division therefore results in a heterogeneous population of progeny. The epithelial compartment of the mammary gland is comprised of luminal epithelial cells and myoepithelial cells, and several studies have identified normal stem-like cells that can generate these different cell types in culture and *in vivo* (16–21).

In contrast to their accepted role in drug efflux (see above), the importance of ABCG2 or the SP as a marker of normal or cancer stem cells is controversial. Evidence against the marker function of SP include the findings that steady-state hematopoiesis is functionally normal in ABCG2 knockout mice (11), that purified mouse mammary SP cells do not efficiently repopulate the mammary gland after injection into cleared fat pads (16), and that normal mammary stem cells in mice do not contain a SP (22, 23). Evidence supporting a marker role for SP cells include the observations that progenitor cells are restricted to the SP fraction of cultured mammospheres (18), that SP abundance is elevated during Wnt-induced mammary oncogenesis in the mouse (24), and that the SP purified from several cancer cell lines show enhanced tumorigenicity *in vivo* relative to their non-SP cohorts (4, 25).

SPs are detectable in several cancer cell lines (4, 10, 25–28), supporting the notion that certain cancers may arise from a cancer stem/progenitor cell. In this report, we characterize the SP in MCF7 breast cancer cells. We show that ABCG2 is responsible for the MCF7 SP, and that the MCF7 SP has properties resembling progenitor cells. Interestingly, ABCG2 expression and SP abundance is strongly repressed during a transforming growth factor-β (TGFβ)–directed epithelial-mesenchymal transition (EMT) and is restored upon reversion of the cells to an epithelial phenotype. The TGFβ-directed EMT also renders MCF7 cells more sensitive to mitoxantrone cytotoxicity. These effects on ABCG2 expression and function result from the EMT-associated repression of *ABCG2* gene expression and a posttranslational inhibition of ABCG2 function mediated by the loss of E-cadherin. Although the extrapolation of results from immortalized cancer cell lines to bone fide stem/progenitor cells must be made with caution, our data suggest that partial EMTs associated with metastasis may control progenitor cell abundance.

Note: Supplementary data for this article are available at Cancer Research Online (http://cancerres.aacrjournals.org/).

Requests for reprints: Richard K. Assoian, Department of Pharmacology, University of Pennsylvania School of Medicine, 3620 Hamilton Walk, Room 167, Philadelphia, PA 19104-6084. Phone: 215-898-7157; Fax: 215-573-5656; E-mail: rka@pharm.med.upenn.edu.

doi:10.1158/0008-5472.CAN-07-2545

Materials and Methods

Cell culture. The human breast cancer cell lines MCF7 and MDA-MB-231 were purchased from American Type Culture Collection and maintained in DMEM supplemented with 10% fetal bovine serum (FBS). For extractions, cells were washed once with ice-cold PBS, split 9:1 into separate tubes for protein and mRNA analysis, collected by centrifugation, quick-frozen, and stored at −80°C prior to analysis.

Flow cytometry and fluorescence-activated cell sorting. SP abundance was determined similarly to the procedure described (13). Cells were trypsinized and washed twice with DMEM supplemented with 2% FBS and 10 mmol/L of HEPES (pH 7.4; DMEM+). For each SP analysis, $\sim 10^6$ cells were resuspended in 1 mL of DMEM+. Hoechst 33342 (1 mg/mL in water; Sigma) was added to a final concentration of 5 μg/mL, and the cells were incubated at 37°C in a water bath for 100 min protected by light and mixed by vortexing every 20 min. To confirm the specificity of the SP signal, duplicate samples were incubated in the presence of fumitremorgin C (FTC; 10 mmol/L in DMSO; Alexis Biochemicals) at a final concentration of 1 μmol/L. At the end of the incubation, all samples were chilled on ice and transferred into microcentrifuge tubes. Cells were washed once with cold HBSS supplemented with 2% FBS and 10 mmol/L HEPES (pH 7.4; HBSS+), resuspended in 1 mL of HBSS+ and transferred to prechilled 5 mL polystyrene tubes (BD Falcon). To assess viability, propidium iodide (1 mg/mL in water; Sigma) was added to a final concentration of 2 μg/mL immediately before running the samples on an LSRII flow cytometer (Becton Dickinson). For cell sorting, ~ 50 to 100×10^6 cells were collected and stained as described above and sorted using a FACS Vantage cell sorter (Becton Dickinson). Sorted SP and non-SP fractions were immediately re-analyzed for purity without further staining.

For surface marker analysis, cells stained with Hoechst 33242 were further incubated (30 min at 4°C) with a 100-fold dilution of anti–ESA-FITC (Biomeda), anti–CD29-FITC (Chemicon), anti–CD24-PE (BD PharMingen), anti–CD44-APC (BD PharMingen), or anti–CD49-PE-Cy5 (BD PharMingen) and then stained with propidium iodide before analysis on the LSRII. For intracellular marker analysis, purified SP and non-SP cells (10^5 cells per 0.1 mL DMEM+) were fixed with 3.7% formaldehyde for 30 min, permeabilized with 0.02% Triton X-100 in PBS (20 min at 4°C), and then incubated (60 min at 4°C) with either anti-cytokeratin 14-FITC (100:1 dilution; Abcam) or anti-cytokeratin 18-FITC (100:1 dilution; Abcam). After washing, the samples were analyzed using a FACS-CALYBER (Becton Dickinson) flow cytometer.

***In vivo* tumorigenicity.** MCF7 cells were infected with a lentivirus encoding green fluorescent protein (GFP) under conditions resulting in ~95% infection. Cells were cultured in DMEM with 10% FBS for several passages and then sorted into GFP^+ SP and GFP^+ non-SP cells by fluorescence-activated cell sorting (FACS). The purified cells were allowed to recover overnight in DMEM with 10% FBS. A selected number of sorted GFP^+ SP and GFP^+ non-SP cells (ranging from 10^2 to 10^5) were resuspended in 25 μL of a DMEM/Matrigel (Matrigel Basement Membrane Matrix; Becton Dickinson) mixture (3:1 v/v) and injected into the fourth mammary fat pad of 8-week-old female nonobese diabetic/severe combined immunodeficiency (NOD/SCID) mice (Jackson Laboratory) that had been anesthetized with Avertin (2.5%, 0.15–0.17 mL/g body weight) by i.p. injection. The animals received a sulfamethoxazole and trimethoprim oral pediatric suspension (5 mL/100 mL of drinking water; Hi-Tech Pharmacal) for 1 week after the surgery. The animals were sacrificed 6 to 7 months after tumor cell injection, and whole mounts of freshly harvested mammary tissue were carefully analyzed by immunofluorescence microscopy for GFP signals as described below but using a Nikon 10×/0.3 Plan Fluor objective. Animal procedures were approved by the University of Pennsylvania Institutional Animal Care and Use Committee.

TGFβ-directed EMT. MCF7 cells in DMEM-10% FBS were seeded at low confluence (3×10^5 cells) in 100-mm dishes containing autoclaved glass coverslips. An incomplete EMT was induced by incubating the MCF7 cells for 3 days in maintenance medium with 10 ng/mL of human recombinant TGFβ1 (R&D Systems). Duplicate cultures were incubated in parallel without TGFβ. Samples were collected for analysis by flow cytometry, immunofluorescence microscopy, Western blotting, and quantitative real-time RT-PCR (QPCR). The amount of TGFβ needed and the duration of treatment was determined by assessing stress fiber formation and loss of E-cadherin–mediated cell-cell adhesion. To reverse the EMT, the transitioned cells were washed, trypsinized, and reseeded into two 100-mm dishes in DMEM-10% FBS, for 10 days. The cells were trypsinized and reseeded at 50% confluence every 3 days.

Mitoxantrone cytotoxicity assay. Exponentially growing MCF7 cells were trypsinized, and replicate cultures were plated in the absence (*Ctrl*) or presence of TGFβ (to induce the EMT) as described above. Control and transitioned cells were then trypsinized and seeded in quadruplicate in 96-well plates at densities of 1,500 and 2,000 cells per well, respectively, in 0.1 mL of DMEM-10% FBS with or without 10 ng/mL of TGFβ. Mitoxantrone (Sigma) was added to the plates at the time of seeding at final concentrations of 0 to 100 nmol/L, and the cultures were incubated at 37°C for 7 days. Sensitivity to the cytotoxic effect of mitoxantrone was assessed using a 3-(4,5-dimethylthiazol-2-yl)-2,5-diphenyltetrazolium bromide assay (Millipore) according to the instructions of the manufacturer. Absorbance was measured at a test wavelength of 570 nm and a reference wavelength of 630 nm for each well using a microplate reader (Dynex Technology). Background absorbance (staining in the absence of cells) was subtracted from each sample before calculating the absorbance ratio (treated cells/untreated cells).

Short interfering RNA knock-down. For short interfering RNA (siRNA) experiments, MCF7 cells (1×10^6 cells) were seeded in 35-mm dishes in maintenance medium without antibiotics the day before transfection. The cells were washed thrice with serum/growth factor–free Optimem (Invitrogen), and then transfected with siRNAs (Ambion) for human ABCG2 (200 nmol/L; GGCAAAUCUUCGUUAUUAGtt or GCCUACAACUGGCUUAGACtt), human E-cadherin (150 nmol/L; GAGUGAAUUUUGAAGAUUGtt or GCACGUACACAGCCCUAAUtt), or irrelevant controls (mouse LIMK1; Ambion GGUAUUGACAGGGAUCUGAtt or mouse Rac1; Ambion CCGUCUUUGACAACUAUUCtt) using 10 μL LipofectAMINE 2000 (Invitrogen) per well. After an overnight incubation, the cells were trypsinized and reseeded from 35- to 100-mm dishes in DMEM-10% FBS for 2 days before analysis.

Immunofluorescence microscopy. Cells were seeded in 100-mm dishes containing autoclaved glass coverslips and cultured in DMEM with 10% FBS. Cells were washed twice with PBS, fixed with 3.7% formaldehyde for 10 min, and then incubated with 50 mmol/L of ammonium chloride for 10 min. Cells were permeabilized and blocked with 0.5% Triton X-100 in PBS with 0.2% bovine serum albumin and 2% goat serum for 30 min at room temperature prior to immunostaining (1 h at 25°C) with anti–E-cadherin at 4 μg/mL (Invitrogen), followed by Alexa Fluor 594 donkey anti-mouse IgG (1:1,000). Filamentous actin (F-actin) was detected using 1.5 units/mL of FITC-conjugated phalloidin, and nuclei were stained with 4,6-diamidino-2-phenylindole (DAPI). Images were obtained by epifluorescence microscopy, captured using a Nikon Eclipse 80i microscope, Leitz 40/0.7 PL FLUOTAR objective, and a Hamamatsu C4742-95 digital camera and camera controller. Images were acquired and converted to TIFF files using Openlab (Improvision) or Image-Pro (Media Cybernetics) software and assembled using Photoshop (Adobe).

QPCR. Total RNA was extracted from cell pellets (10% of sample; ~ 4–6×10^5 cells per 100-mm dish) using 0.5 mL of TRIzol (Invitrogen) as directed by the manufacturer's instructions. Reverse transcription was done in 10-μL reactions on 100 to 150 ng total RNA from each sample using Applied Biosystems Reverse Transcription Reagents (5.5 mmol/L $MgCl_2$, 2 mmol/L deoxynucleotide triphosphate, 2.5 μmol/L random hexamers, 0.4 units/μL RNase inhibitor, and 1.25 units/μL Multiscribe Reverse Transcriptase) as directed by the manufacturer's instructions. For QPCR, duplicate aliquots of cDNA for each sample (2 μL) were then subjected to 40 amplification cycles of PCR (Applied Biosystems Prism 7000 sequence detection system) using TaqMan Universal PCR Master Mix and primer-probe sets for 18S rRNA (29) or human ABCG2 (900 nmol/L forward primer TGC AAC AGG AAA CAA TCC TTG T, 900 nmol/L reverse primer AGA TCG ATG CCC TGC TTT ACC, and 250 nmol/L probe 6FAM CAA CAT GTA CTG GCG AAG A-MGBNFQ). RNA expression was quantified by a standard curve

using ABI Prism 7000 sequence detection system software. QPCR results are plotted as the relative levels of ABCG2 mRNA normalized to 18S rRNA and expressed as mean ± SD of the duplicate PCR reactions.

Western blot analysis. Western blotting was done as described (30) using 50 μg (1.5 × 8 × 7.3 cm gel) or 100 μg (1.5 × 14 × 15 cm gel) of total cellular protein and the following antibodies: ABCG2 (Chemicon), cdk4 (AHZ0202; Biosource), and E-cadherin (13-1700; Invitrogen). Western blots were visualized using enhanced chemiluminescence (Amersham), digitized by scanning, and assembled in Photoshop.

Results

ABCG2 is responsible for the MCF7 SP. Others have described a SP in MCF7 cells which expresses ABCG2 mRNA (25). We confirmed the presence of a SP in MCF7 cells (Fig. 1*A; MCF7*) and found enhanced expression of both ABCG2 mRNA and protein in purified SP cells relative to non-SP cells (Fig. 1*B* and *C*, respectively). Semiquantitative RT-PCR showed that MCF7 cells did not express MDR1 mRNA, and 25 to 50 μmol/L of verapamil which inhibits MDR1—but not ABCG2 (6, 8)—did not affect the abundance of the MCF7 SP (data not shown). In contrast, 1 μmol/L of the ABCG2-specific inhibitor, FTC (31, 32), eliminated the MCF7 SP (Fig. 1*A*; *FTC*). Similarly, two distinct ABCG2 siRNAs strongly reduced SP abundance (Fig. 1*A*; *siRNA1* and *siRNA2*), to 13.5 ± 2.8% (mean ± SE, n = 8) of that seen with an irrelevant siRNA. We conclude that ABCG2 is responsible for the SP in MCF7 cells.

Purified MCF7 SP cells generate a heterogeneous population of both SP and non-SP cells. We purified MCF7 SP and non-SP cells and assessed their ability to regenerate SP and non-SP fractions during their time in culture. The initial SP and non-SP fractions were 93% and 96% pure as determined by flow cytometry (Fig. 2*A*). We then grew both purified populations in culture for 2 weeks and re-analyzed them for Hoechst 33342 efflux by flow cytometry. The SP gave rise to a mixed population of SP and non-SP (Fig. 2*B*; 2.55% *SP*) which closely resembled the percentages of SP and non-SP cells seen in unsorted MCF7 cells (0.7–2.0%, n = 12). In contrast, the purified non-SP cells did not generate SP cells during the experiment (Fig. 2*B*; *NSP*). The ability of the purified MCF7 SP to generate both SP and non-SP cells has also been observed for the SPs of certain neuroblastoma, glioma, and lung cancer cell lines (4, 10, 28) and may be related to the asymmetrical cell division that is characteristic of stem and cancer stem cells (see Discussion).

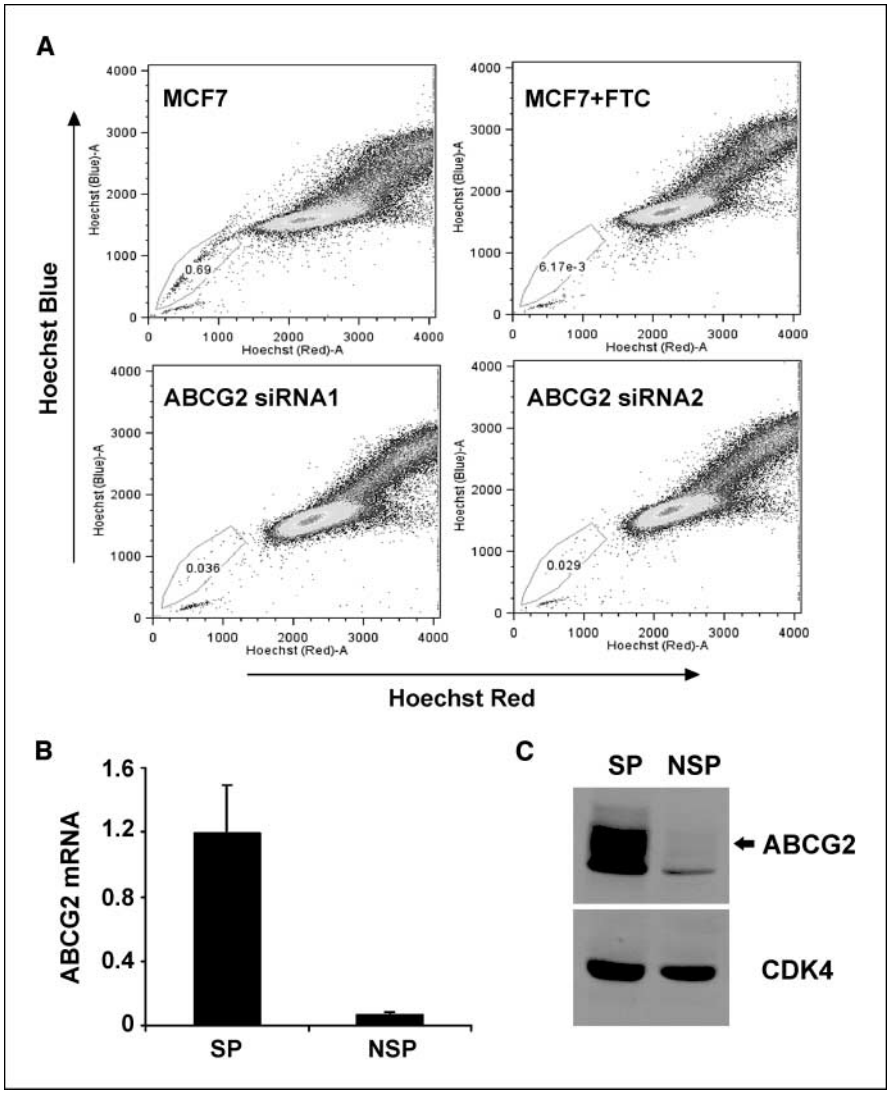

Figure 1. ABCG2 is responsible for the MCF7 SP. *A,* exponentially growing MCF7 cells were stained with Hoechst 33342 in the absence (*top left*) or presence (*top right*) of 1 μmol/L of FTC. MCF7 cells were also transfected with control siRNAs (data not shown, but refer to Fig. 5*B*) or two distinct ABCG2 siRNAs before staining with Hoechst (*bottom left* and *bottom right*). Refer to Fig. 5*D* for representative knock-down efficiencies. The cells were analyzed by flow cytometry as described in Materials and Methods. The SP regions are encircled. *B* and *C,* exponentially growing MCF7 cells were collected, lysed, and analyzed by QPCR and Western blotting, respectively, for ABCG2 mRNA and protein in purified SP and non-SP (*NSP*) cells. ABCG2 mRNA levels are plotted relative to 18S rRNA. CDK4 serves as a loading control for the Western blot.

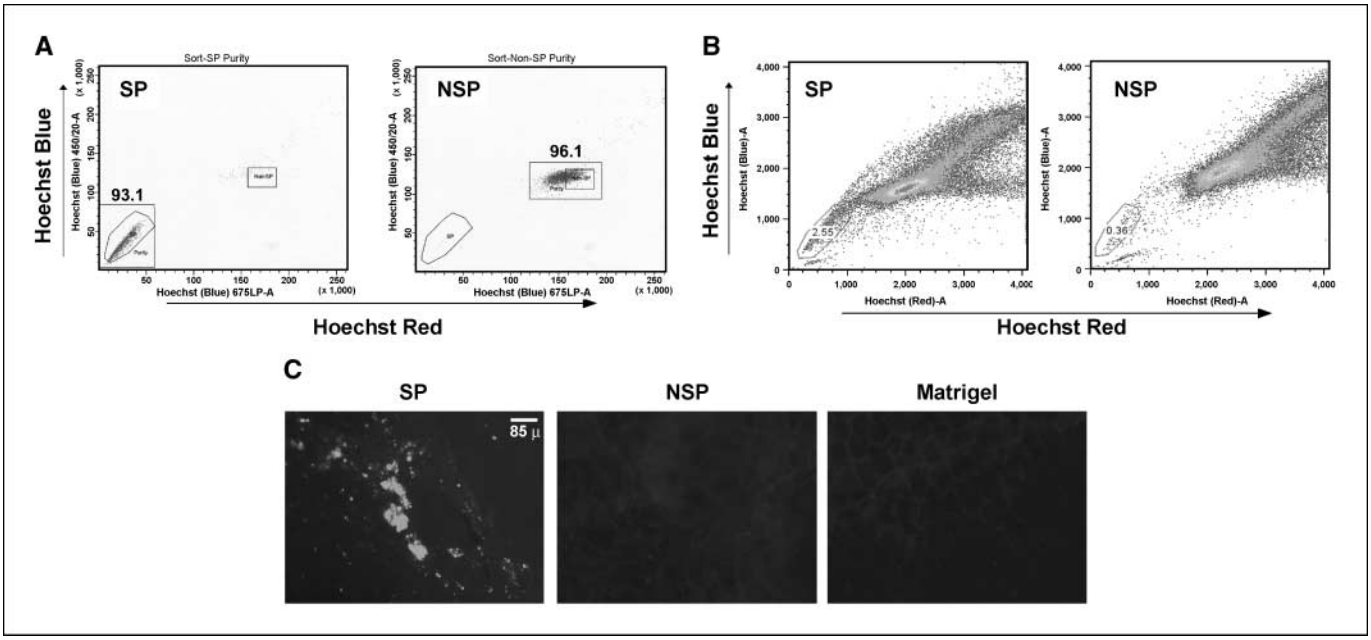

Figure 2. Properties of MCF7 SP and non-SP cells. *A,* exponentially growing MCF7 SP and non-SP (*NSP*) fractions were purified by FACS as described in Materials and Methods and then immediately re-analyzed by flow cytometry for purity (% SP and non-SP). *B,* purified SP and NSP MCF7 cells were seeded (7×10^5 cells in 60-mm dish) and incubated in DMEM-10% FBS for 14 d (trypsinizing and reseeding at ~50% subconfluence as needed to avoid confluence). The cells were then re-stained with Hoechst 33342, and re-analyzed by flow cytometry. The SP regions are encircled. *C,* GFP-positive MCF7 SP and NSP cells were purified by FACS and injected into the mammary glands of NOD/SCID mice as described in Materials and Methods. Representative images of GFP-positive cells in whole mounts prepared 7 mo after injection of 1×10^4 cells (GFP^+ SP, GFP^+ NSP) and vehicle (Matrigel) alone.

We then compared the expression of lineage markers in SP and non-SP MCF7 cells (Supplemental Fig. S1*A*). Both the SP and non-SP fractions displayed a luminal mammary epithelial phenotype as determined by expression of ESA and cytokeratin 18, and the absence of cytokeratin 14 (19, 20). Expression of the putative stem cell markers CD24, CD44, CD29, and CD49 (22, 23, 33) was also similar in the two subpopulations with both cell populations being $CD24^+/CD44^{low}/CD29^{low}/CD49^+$ (Supplemental Fig. S1*B*). Thus, the difference in the cell division properties of SP and non-SP cells does not reflect a fundamental difference in their cell lineage.

Tumorigenic potential of the MCF7 SP. To compare the tumorigenic potential of the MCF SP and non-SP, MCF7 cells were infected with a lentivirus encoding GFP and pure GFP-positive SP and non-SP fractions were purified by FACS. A selected number of cells were injected into the fourth mammary fat pad of 8-week-old NOD/SCID female mice and were monitored for tumor development. Consistent with the weak tumorigenicity of MCF7 cells (34), we did not detect palpable tumors in the mice. However, when whole mounts of collected mammary glands were analyzed by fluorescence microscopy, it became clear that the MCF7 SP cells efficiently colonized the mammary glands (11 occurrences of 26 total injections). In contrast, non-SP cells colonized the mammary gland in only 2 of 25 injections. Representative images are shown in Fig. 2*C*, and the complete analysis is summarized in Supplemental Table S1.

Repression of *ABCG2* gene expression and SP abundance by a TGFβ-directed EMT. The EMT is a reprogramming of epithelial cells that results in their modulation to a mesenchymal phenotype (35–37). This change in phenotype is typically accompanied by loss of E-cadherin–mediated cell-cell adhesion and an increase in mesenchymal markers such as actin stress fibers (a marker of increased cellular tension). The EMT has an established role in promoting cell migration during development, and it may also promote migration during the metastasis of cancer cells (35–37). EMTs have been categorized as either incomplete (reversible) or complete (irreversible; refs. 36, 37). TGFβ is a well-characterized inducer of the EMT (38–41), and previous studies have indicated that exposure of cells to TGFβ (in the absence of a cooperating Ras oncogene) results in a reversible EMT (42).

To determine if *ABCG2* gene expression and SP abundance are regulated during the EMT, we treated MCF7 cells with TGFβ and induced an EMT-like phenotype as assessed by loss of cell surface E-cadherin, disruption of cell-cell contacts, and acquisition of fibroblast-like morphology with increased cell spreading and detectable stress fibers (Supplemental Fig. S2). These transitioned cells had a striking decrease in SP abundance (Fig. 3*A*; *MCF7; Ctrl* versus *EMT*). Reduction of the SP was accompanied by repression of ABCG2 mRNA (Fig. 3*B, MCF7*; Supplemental Fig. S2) and protein expression (Fig. 3*C, MCF7*; Supplemental Fig. S2). The same effects were seen when purified MCF7 SP cells were treated with TGFβ (Fig. 3*A–C*; *SP*). Moreover, when TGFβ was withdrawn from the transitioned cells, they reverted to the epithelial phenotype (also called a mesenchymal-epithelial transition) over a 10-day period as assessed by the reappearance of E-cadherin–based cell-cell adhesions (Fig. 4*A*). Reversion to the epithelial phenotype restored full expression of ABCG2 (Fig. 4*B*) and the SP (Fig. 4*C*). Thus, *ABCG2* gene expression and SP abundance are strongly inhibited during the partial EMT induced by TGFβ in MCF7 cells.

The presence of an ABCG2-dependent SP is associated with increased resistance to certain chemotherapeutic drugs, one of

which is mitoxantrone (2). To assess the functional consequence of the EMT-associated decrease in ABCG2 expression and SP abundance, we compared the resistance of MCF7 cells to mitoxantrone toxicity before and after the TGFβ-induced EMT. The IC_{50} of mitoxantrone was decreased 5-fold after the EMT (Fig. 3*D*), with an average decrease in IC_{50} of 7 ± 1.5 (mean ± SE, n = 3). Thus, the EMT-associated decrease in ABCG2 expression and SP abundance results in an increased sensitivity to mitoxantrone.

E-cadherin depletion reduces SP abundance without affecting ABCG2 expression. To assess the mechanism by which the TGFβ-directed EMT regulates ABCG2 expression and SP abundance, we first assessed the potential effect of altering cellular tension. We plated MCF7 cells on a malleable collagen-coated surface which allowed us to manipulate substrate stiffness and thereby alter cellular tension (29, 43). We then examined the effect of changes in cellular tension on SP abundance. However, changes in cellular tension did not affect SP abundance (Supplemental Fig. S3).

We then asked if E-cadherin depletion in control MCF7 cells would phenocopy the effects seen after the TGFβ-directed EMT. E-cadherin knock-down with siRNA (Fig. 5*A* and *D*) decreased SP abundance, although the magnitude of this effect was less than that seen after the EMT or after knock-down of ABCG2 itself (Fig. 5*B*). In eight determinations with two distinct siRNAs, E-cadherin knock-down reduced SP abundance to 44 ± 3.4% (mean ± SE) of control (irrelevant siRNA), whereas the TGFβ-directed EMT reduced SP abundance to 3.8 ± 1.5% (mean ± SE, n = 8) of control (untreated) cells. Importantly, the effect of E-cadherin knock-down on SP abundance occurred despite a minimal effect on ABCG2 mRNA and protein expression (Fig. 5*C* and *D*, respectively). Thus, in contrast to the repression of *ABCG2* gene expression seen during the TGFβ-directed EMT, E-cadherin knock-down exerts a posttranslational inhibitory effect on ABCG2 function.

The distinct effects of the TGFβ-directed EMT and E-cadherin depletion in MCF7 cells strongly suggested that SP abundance could be regulated by posttranslational effects on ABCG2

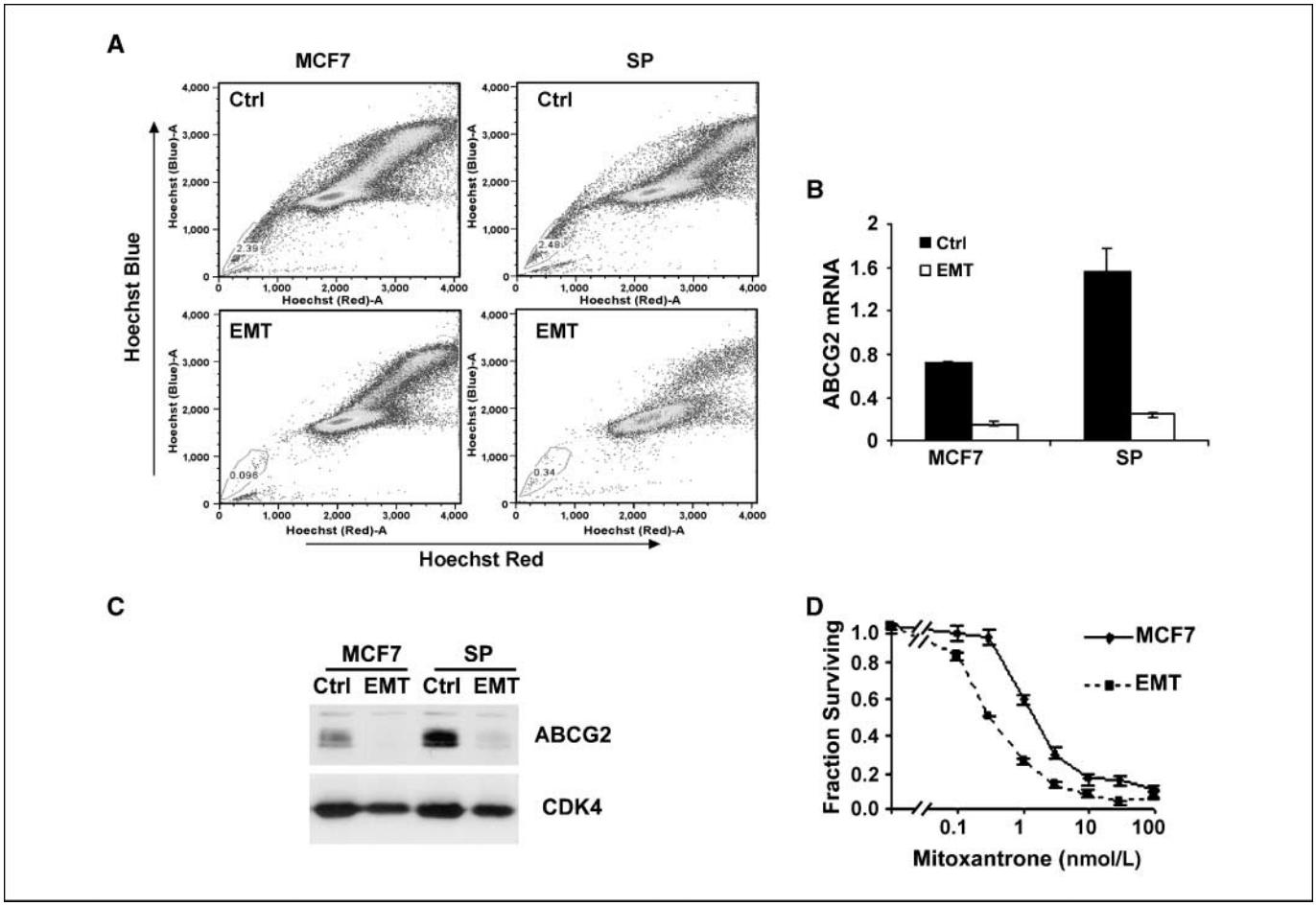

Figure 3. TGFβ-directed EMT down-regulates ABCG2 expression, depletes the SP, and results in increased sensitivity to mitoxantrone. *A,* exponentially growing MCF7 cells or purified SP cells were cultured at 3×10^5 cells per 100-mm dish in DMEM with 10% FBS in the absence or presence of 10 ng/mL of TGFβ for 3 d to induce the EMT. The cells were then stained with Hoechst 33342 and analyzed for SP abundance as described in Materials and Methods. *B* and *C,* control and transitioned MCF7 cells or purified SP cells were analyzed for ABCG2 mRNA and protein, by QPCR and Western blotting, respectively. ABCG2 mRNA levels were plotted relative to 18S rRNA (*B*). CDK4 serves as the loading control (*C*). *D,* exponentially growing MCF7 cells were trypsinized and replicate cultures were plated at 3×10^5 in 100-mm dishes in DMEM with 10% FBS in the absence (*Ctrl*) or presence of TGFβ for 3 d. The control and transitioned cells were then treated for 7 d with mitoxantrone in the continued absence or presence of TGFβ. The medium for each culture condition was replaced at day 4. The cultures were incubated with 3-(4,5-dimethylthiazol-2-yl)-2,5-diphenyltetrazolium bromide, and the results were plotted as the absorbance ratios of treated cell/untreated cells (see Materials and Methods). *Points,* mean from an experiment done in quadruplicate; *bars,* SD. Mitoxantrone concentrations are plotted on log scale.

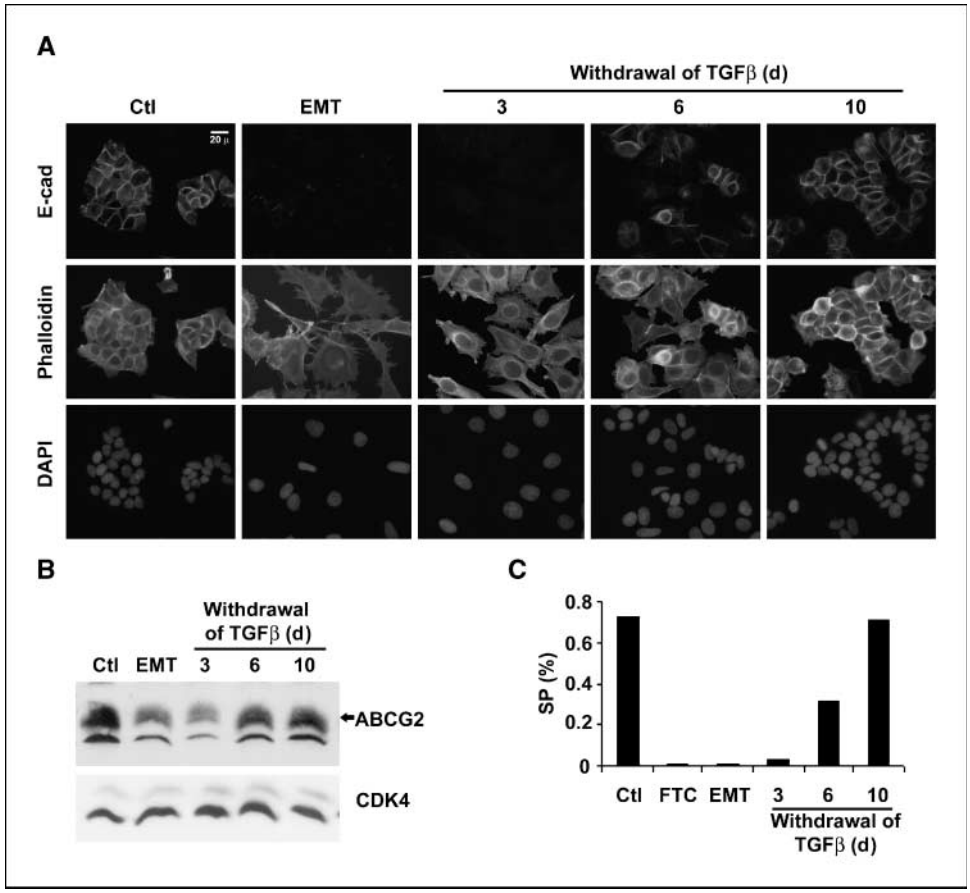

Figure 4. Withdrawal of TGFβ reverses the EMT and restores the SP in MCF7 cells. Exponentially growing MCF7 cells were trypsinized, and replicate cultures were plated at 3×10^5 in 100-mm dishes in DMEM with 10% FBS in the absence (*Ctrl*) or presence of TGFβ for 3 d. TGFβ was then removed from the transitioned cells; reversal of the EMT and restoration of the epithelial phenotype were monitored. *A,* coverslips collected 0 to 10 d after removal of TGFβ (and control MCF7 cells) were analyzed by epifluorescence microscopy after immunostaining for E-cadherin, staining for F-actin with FITC-phalloidin, and staining of nuclei with DAPI. *B,* replicate cultures were collected for analysis of ABCG2 protein levels by Western blotting. Cdk4 serves as the loading control. *C,* replicate cultures were analyzed by FACS to determine SP abundance. *C,* abundance after treating MCF7 cells with the ABCG2 inhibitor, FTC.

function as well as by effects on *ABCG2* gene expression. To determine if posttranslational regulation of ABCG2 function was specific to MCF7 cells, we examined several breast cancer cell lines. Consistent with the report by others (25), we found that MDA-MB-231 cells also lacked a SP (Fig. 6*A*), despite the expression of ABCG2 (Fig. 6*B* and *C*). Importantly, MDA-MB-231 cells lack E-cadherin as determined by Western blotting (Fig. 6*C*) and immunofluorescence microscopy (Fig. 6*D*). Thus, posttranslational regulation of ABCG2 function is linked to E-cadherin expression in at least two distinct experimental settings.

Discussion

Properties of the ABCG2-dependent SP in MCF7 cells. Our study describes the properties and regulation of the ABCG2-dependent SP in MCF7 cells. The analysis of purified MCF7 SP and non-SP fractions showed that the MCF7 SP alone has the ability to generate both SP and non-SP cells and thereby reconstitute the heterogeneous distribution of these subpopulations that is characteristic of the original culture. Further studies will be required to determine how the generation of heterogeneity within this immortalized cell line relates to the stem cell and cancer stem cell property of asymmetrical cell division. Another characteristic of cancer stem cells is enhanced tumorigenicity *in vivo* (44), and we found that only the SP fraction efficiently colonized the mammary gland. Others have reported increased tumorigenicity of the MCF7 SP as compared with the non-SP fraction but used i.p. injection (25). Our study shows enhanced colonization by the SP *in vivo* when injected in the orthotopic site.

Regulation of ABCG2 and SP abundance by a TGFβ-directed EMT. TGFβ is thought to be a suppressor of early tumor formation, but it is also thought to promote the late stages of cancer by stimulating an EMT which, in turn, is associated with extravasation and metastasis (40). Our studies show that *ABCG2* gene expression is strongly repressed by the TGFβ-directed EMT. These effects are reversible because ABCG2 expression and the SP reappear when TGFβ is removed and the transitioned cells undergo a mesenchymal-epithelial transition to regain their epithelial phenotype. Although our results are consistent with the reversibility of TGFβ-directed EMT, we cannot exclude the possibility that the reduction in ABCG2 expression seen during the TGFβ-directed EMT may reflect a selective inhibition of cell division within the SP subpopulation. Indeed, TGFβ is thought to regulate stem/progenitor cell differentiation (45). If this is the case, MCF7 cells subjected to a TGFβ-directed EMT must be less differentiated than purified non-SP cells because the EMT-like cells can revert to a phenotype that re-expresses ABCG2 and a functional SP.

Because the EMT is associated with late stages and aggressiveness of cancer, it may seem counterintuitive for transitioned MCF7 cells to show decreased ABCG2 expression and an increased sensitivity to ABCG2-effluxed chemotherapeutic drugs. Although the extrapolation of results from immortalized cancer cell lines to bone fide cancer cells must be made with caution, our results imply that a transient therapeutic window

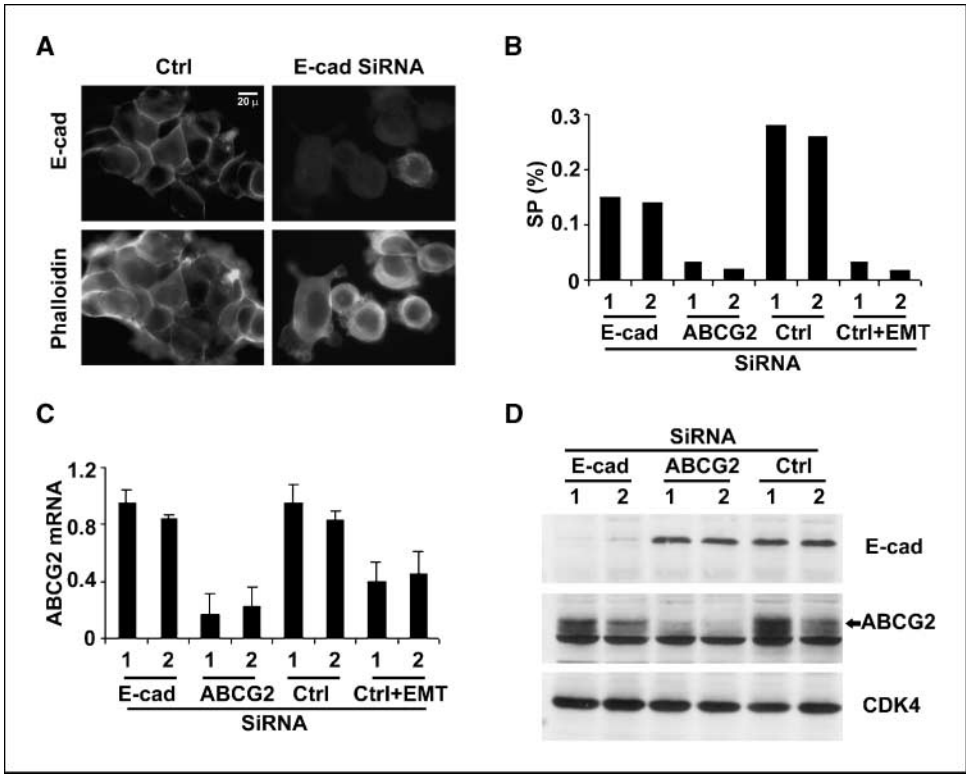

Figure 5. Posttranslational regulation of ABCG2 function by E-cadherin. Exponentially growing MCF7 cells (10^6) were plated in six-well plates and transfected with control or E-cadherin siRNAs. *A,* cultures were incubated in DMEM-10% FBS for 2.5 d after transfection; collected coverslips were analyzed for the expression of E-cadherin and F-actin by epifluorescence microscopy. Representative images for control siRNA (mLIMK1) and E-cadherin siRNA-1. *B* to *D,* MCF7 cells transfected with control siRNAs, ABCG2 siRNAs, or E-cadherin siRNAs. Cells transfected with control siRNAs were also incubated in the absence (*Ctrl*) or presence of 10 ng/mL of TGFβ (*Ctrl + EMT*) for the 2.5-d period after transfection. *B,* the percentage of SP cells in each population as determined by flow cytometry. *C,* the levels of ABCG2 mRNA as determined by QPCR; ABCG2 mRNA levels are plotted relative to 18S rRNA. *D,* Western blots of collected cell lysates probed for E-cadherin (*E-cad*), ABCG2, and CDK4 (loading control). In three separate experiments, the two E-cadherin siRNAs did not have any reproducible effect on ABCG2 levels.

may exist as tumor cells undergo an EMT and before they revert to the epithelial phenotype at distal sites. Alternatively, because ABCG2 inhibits hypoxia-associated cell death (9), down-regulation of ABCG2 during the TGFβ-directed EMT may sensitize tumor cells to hypoxic death signals and thereby contribute to the low efficiency of metastasis formation (46). Given the potential relationship between the SP and cancer stem/progenitor cells (4, 24, 25), our data also raises the possibility that the cancer stem/progenitor population is transiently repressed during the EMT and reappears after the colonization of secondary sites and reversion of tumor cells to the epithelial phenotype. It is important to emphasize, however, that the ABCG2-dependent SP is not a consistent marker of stem cells (11, 16, 22, 23), and that the relationship between the SP and the biology of cancer stem cells is not well understood.

Posttranslational regulation of ABCG2 function by E-cadherin. A hallmark of the EMT is loss of E-cadherin–dependent cell-cell adhesions, and we find that knock-down of E-cadherin decreases SP abundance as does the TGFβ-directed EMT. The effect of E-cadherin knock-down is less complete than that seen with TGFβ-directed EMT. More importantly, however, E-cadherin depletion reduces SP abundance despite the

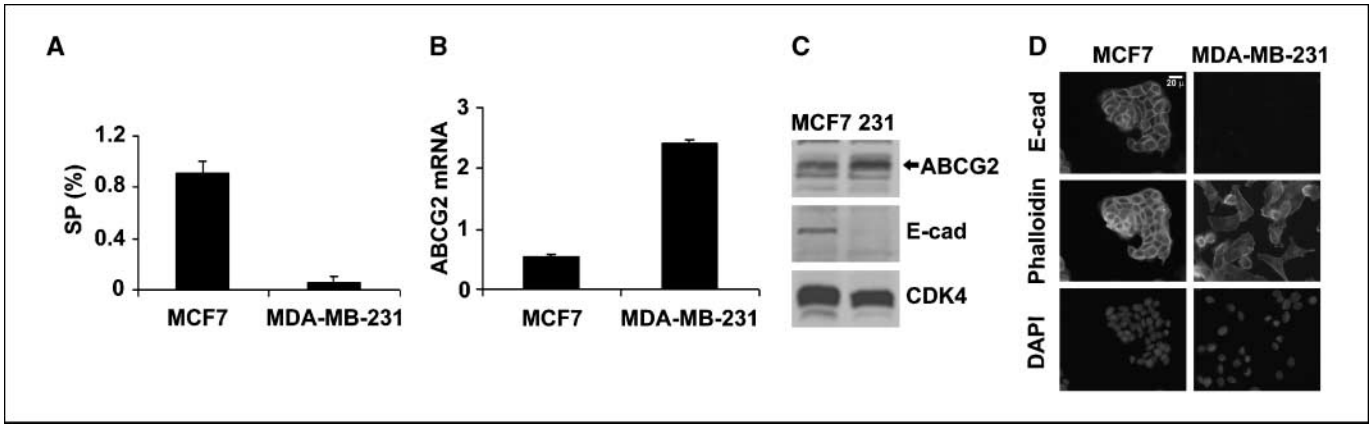

Figure 6. Posttranslational regulation of SP abundance in MDA-MB-231 cells. *A,* exponentially growing MCF7 and MDA-MB-231 cells were trypsinized and stained with Hoechst 33342 and then analyzed for SP abundance by flow cytometry. *Columns,* mean; *bars,* SE ($n = 4$). *B,* exponentially growing MCF7 and MDA-MB-231 cells were analyzed for ABCG2 mRNA by QPCR. ABCG2 mRNA levels were plotted relative to 18S rRNA. *C,* exponentially growing MCF7 and MDA-MB-231 cells were analyzed by Western blotting for ABCG2, E-cadherin, and CDK4 (loading control). *D,* MCF7 and MDA-MB-231 cells were stained with anti–E-cadherin, FITC-phalloidin, and DAPI, and analyzed by epifluorescence microscopy.

persistence of the ABCG2 protein. This posttranslational regulation of ABCG2 function by E-cadherin cooperates with the transcriptional repression of the *ABCG2* gene to prevent ABCG2 transporter function during the TGFβ-directed EMT. Interestingly, MDA-MB-231 cells (which also lack a SP despite the expression of ABCG2) do not express E cadherin, suggesting that posttranslational regulation of ABCG2 function as a transporter may be a common effect of E-cadherin signaling. Because ABCG2 is a half-transporter (2, 6), assembly of the functional homodimer and its localization to the plasma membrane may be regulated processes. Posttranslational regulation of ABCG2 function may explain why purified SP and ABCG2-positive cells have different tumorigenic potentials *in vivo* (25).

Acknowledgments

Received 7/1/2007; revised 10/15/2007; accepted 12/6/2007.

Grant support: Breast Cancer Alliance and NIH grant CA72639.

The costs of publication of this article were defrayed in part by the payment of page charges. This article must therefore be hereby marked *advertisement* in accordance with 18 U.S.C. Section 1734 solely to indicate this fact.

We thank Charlotte Kuperwasser for training in the *in vivo* tumorigenicity experiment and Eric Klein for assistance in the preparation and use of the malleable substrata.

References

1. Lepper ER, Nooter K, Verweij J, Acharya MR, Figg WD, Sparreboom A. Mechanisms of resistance to anticancer drugs: the role of the polymorphic ABC transporters ABCB1 and ABCG2. Pharmacogenomics 2005;6:115–38.
2. Doyle LA, Ross DD. Multidrug resistance mediated by the breast cancer resistance protein BCRP (ABCG2). Oncogene 2003;22:7340–58.
3. Bunting KD. ABC transporters as phenotypic markers and functional regulators of stem cells. Stem Cells 2002;20:11–20.
4. Ho MM, Ng AV, Lam S, Hung JY. Side population in human lung cancer cell lines and tumors is enriched with stem-like cancer cells. Cancer Res 2007;67:4827–33.
5. Yoshikawa M, Ikegami Y, Hayasaka S, et al. Novel camptothecin analogues that circumvent ABCG2-associated drug resistance in human tumor cells. Int J Cancer 2004;110:921–7.
6. Litman T, Brangi M, Hudson E, et al. The multidrug-resistant phenotype associated with overexpression of the new ABC half-transporter, MXR (ABCG2). J Cell Sci 2000;113:2011–21.
7. Doyle LA, Yang W, Abruzzo LV, et al. A multidrug resistance transporter from human MCF-7 breast cancer cells. Proc Natl Acad Sci U S A 1998;95:15665–70.
8. Ozvegy C, Litman T, Szakacs G, et al. Functional characterization of the human multidrug transporter, ABCG2, expressed in insect cells. Biochem Biophys Res Commun 2001;285:111–7.
9. Krishnamurthy P, Ross DD, Nakanishi T, et al. The stem cell marker Bcrp/ABCG2 enhances hypoxic cell survival through interactions with heme. J Biol Chem 2004;279:24218–25.
10. Hirschmann-Jax C, Foster AE, Wulf GG, et al. A distinct "side population" of cells with high drug efflux capacity in human tumor cells. Proc Natl Acad Sci U S A 2004;101:14228–33.
11. Zhou S, Morris JJ, Barnes Y, Lan L, Schuetz JD, Sorrentino BP. Bcrp1 gene expression is required for normal numbers of side population stem cells in mice, and confers relative protection to mitoxantrone in hematopoietic cells *in vivo*. Proc Natl Acad Sci U S A 2002;99:12339–44.
12. Zhou S, Schuetz JD, Bunting KD, et al. The ABC transporter Bcrp1/ABCG2 is expressed in a wide variety of stem cells and is a molecular determinant of the side-population phenotype. Nat Med 2001;7:1028–34.
13. Goodell MA, Brose K, Paradis G, Conner AS, Mulligan RC. Isolation and functional properties of murine hematopoietic stem cells that are replicating *in vivo*. J Exp Med 1996;183:1797–806.
14. Reya T, Morrison SJ, Clarke MF, Weissman IL. Stem cells, cancer, and cancer stem cells. Nature 2001;414:105–11.
15. Al-Hajj M, Becker MW, Wicha M, Weissman I, Clarke MF. Therapeutic implications of cancer stem cells. Curr Opin Genet Dev 2004;14:43–7.
16. Alvi AJ, Clayton H, Joshi C, et al. Functional and molecular characterisation of mammary side population cells. Breast Cancer Res 2003;5:R1–8.
17. Clayton H, Titley I, Vivanco M. Growth and differentiation of progenitor/stem cells derived from the human mammary gland. Exp Cell Res 2004;297:444–60.
18. Dontu G, Abdallah WM, Foley JM, et al. *In vitro* propagation and transcriptional profiling of human mammary stem/progenitor cells. Genes Dev 2003;17:1253–70.
19. Gudjonsson T, Villadsen R, Nielsen HL, Ronnov-Jessen L, Bissell MJ, Petersen OW. Isolation, immortalization, and characterization of a human breast epithelial cell line with stem cell properties. Genes Dev 2002;16:693–706.
20. Welm B, Behbod F, Goodell MA, Rosen JM. Isolation and characterization of functional mammary gland stem cells. Cell Prolif 2003;36 Suppl 1:17–32.
21. Welm BE, Tepera SB, Venezia T, Graubert TA, Rosen JM, Goodell MA. Sca-1(pos) cells in the mouse mammary gland represent an enriched progenitor cell population. Dev Biol 2002;245:42–56.
22. Stingl J, Eirew P, Ricketson I, et al. Purification and unique properties of mammary epithelial stem cells. Nature 2006;439:993–7.
23. Shackleton M, Vaillant F, Simpson KJ, et al. Generation of a functional mammary gland from a single stem cell. Nature 2006;439:84–8.
24. Liu BY, McDermott SP, Khwaja SS, Alexander CM. The transforming activity of Wnt effectors correlates with their ability to induce the accumulation of mammary progenitor cells. Proc Natl Acad Sci U S A 2004;101:4158–63.
25. Patrawala L, Calhoun T, Schneider-Broussard R, Zhou J, Claypool K, Tang DG. Side population is enriched in tumorigenic, stem-like cancer cells, whereas ABCG2+ and ABCG2− cancer cells are similarly tumorigenic. Cancer Res 2005;65:6207–19.
26. Wulf GG, Wang RY, Kuehnle I, et al. A leukemic stem cell with intrinsic drug efflux capacity in acute myeloid leukemia. Blood 2001;98:1166–73.
27. Feuring-Buske M, Hogge DE. Hoechst 33342 efflux identifies a subpopulation of cytogenetically normal CD34(+)CD38(-) progenitor cells from patients with acute myeloid leukemia. Blood 2001;97:3882–9.
28. Kondo T, Setoguchi T, Taga T. Persistence of a small subpopulation of cancer stem-like cells in the C6 glioma cell line. Proc Natl Acad Sci U S A 2004;101:781–6.
29. Klein EA, Yung Y, Castagnino P, Kothapalli D, Assoian RK. Cell adhesion, cellular tension and cell cycle control. Methods Enzymol 2007;426:155–75.
30. Welsh CF, Roovers K, Villanueva J, Liu Y, Schwartz MA, Assoian RK. Timing of cyclin D1 expression within G1 phase is controlled by Rho. Nat Cell Biol 2001;3:950–7.
31. Rabindran SK, Ross DD, Doyle LA, Yang W, Greenberger LM. Fumitremorgin C reverses multidrug resistance in cells transfected with the breast cancer resistance protein. Cancer Res 2000;60:47–50.
32. Allen JD, van Loevezijn A, Lakhai JM, et al. Potent and specific inhibition of the breast cancer resistance protein multidrug transporter *in vitro* and in mouse intestine by a novel analogue of fumitremorgin C. Mol Cancer Ther 2002;1:417–25.
33. Al-Hajj M, Wicha MS, Benito-Hernandez A, Morrison SJ, Clarke MF. Prospective identification of tumorigenic breast cancer cells. Proc Natl Acad Sci U S A 2003;100:3983–8.
34. White AC, Levy JA, McGrath CM. Site-selective growth of a hormone-responsive human breast carcinoma in athymic mice. Cancer Res 1982;42:906–12.
35. Grunert S, Jechlinger M, Beug H. Diverse cellular and molecular mechanisms contribute to epithelial plasticity and metastasis. Nat Rev Mol Cell Biol 2003;4:657–65.
36. Thiery JP. Epithelial-mesenchymal transitions in tumour progression. Nat Rev Cancer 2002;2:442–54.
37. Thiery JP. Epithelial-mesenchymal transitions in development and pathologies. Curr Opin Cell Biol 2003;15:740–6.
38. Zavadil J, Bottinger EP. TGF-β and epithelial-to-mesenchymal transitions. Oncogene 2005;24:5764–74.
39. Bhowmick NA, Ghiassi M, Bakin A, et al. Transforming growth factor-β1 mediates epithelial to mesenchymal transdifferentiation through a RhoA-dependent mechanism. Mol Biol Cell 2001;12:27–36.
40. Bierie B, Moses HL. Tumour microenvironment: TGFβ: the molecular Jekyll and Hyde of cancer. Nat Rev Cancer 2006;6:506–20.
41. Miettinen PJ, Ebner R, Lopez AR, Derynck R. TGF-β induced transdifferentiation of mammary epithelial cells to mesenchymal cells: involvement of type I receptors. J Cell Biol 1994;127:2021–36.
42. Gal A, Sjoblom T, Fedorova L, Imreh S, Beug H, Moustakas A. Sustained TGFβ exposure suppresses Smad and non-Smad signalling in mammary epithelial cells, leading to EMT and inhibition of growth arrest and apoptosis. Oncogene. Epub 2007 Aug 27.
43. Yeung T, Georges PC, Flanagan LA, et al. Effects of substrate stiffness on cell morphology, cytoskeletal structure, and adhesion. Cell Motil Cytoskeleton 2005;60:24–34.
44. Pardal R, Clarke MF, Morrison SJ. Applying the principles of stem-cell biology to cancer. Nat Rev Cancer 2003;3:895–902.
45. Mishra L, Derynck R, Mishra B. Transforming growth factor-β signaling in stem cells and cancer. Science 2005;310:68–71.
46. Steeg PS. Tumor metastasis: mechanistic insights and clinical challenges. Nat Med 2006;12:895–904.